Industrial Crops & Products 198 (2023) 116656

Contents lists available at ScienceDirect

Industrial Crops & Products

journal homepage: www.elsevier.com/locate/indcrop

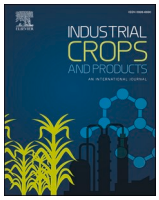

Effects of pH and temperature of ultrafiltration on the composition and physicochemical properties of hot-water-extracted softwood galactoglucomannans

Abedalghani Halahlah [a,1], Felix Abik [a,1], Maarit H. Lahtinen [a], Asmo Kemppinen [a], Kalle Kaipanen [c], Petri O. Kilpeläinen [c], Daniel Granato [d], Thao M. Ho [a,b], Kirsi S. Mikkonen [a,b,*]

[a] Department of Food and Nutrition, University of Helsinki, P.O. Box 66, FIN-00014 Helsinki, Finland
[b] Helsinki Institute of Sustainability Science (HELSUS), University of Helsinki, P.O. Box 65, FIN-00014 Helsinki, Finland
[c] Biorefinery and Bioproducts, Production Systems Unit - Natural Resources Institute Finland (Luke), Viikinkaari 9, FI-00790 Helsinki, Finland
[d] Bioactivity and Applications Lab, Department of Biological Sciences, University of Limerick, Limerick V94 T9PX, Ireland

ARTICLE INFO

Keywords:
Galactoglucomannans
Ultrafiltration
Acetylation degree
Membrane concentration
Physicochemical characterization

ABSTRACT

The recovery of softwood galactoglucomannans (GGM) by pressurized hot water extraction and further concentration by membrane filtration followed by spray drying yield biopolymers suitable as raw materials for renewable products. GGM are often characterized as having low viscosity in water and excellent emulsion stabilizing capacity, enhanced by lignin structures co-extracted with GGM. To reduce membrane fouling during filtration and subsequently to increase product yield, the pH and temperature of GGM liquor can be increased, but effects of such conditions on properties of recovered GGM have not been well understood. Herein, we systematically varied the ultrafiltration pH (6–10) and temperature (30–60 °C) and characterized the composition and physicochemical properties of spray-dried GGM powders in comparison with freeze-dried (fGGM) and ethanol precipitated GGM (eGGM). The GGM samples ultrafiltrated at 60 °C and pH 10 (GGM-10/60) showed lower molar mass (2200 Da), degree of acetylation (0.09) and absolute ζ-potential (13 mV) than the other ultrafiltrated samples at pH (6–10) and temperature (30–45 °C) (3200–3700 Da, 0.11–0.15 and 23–32 mV, respectively). These differences could explain the unique gel formation capacity of GGM-10/60 after ultrasonication, which opens new prospects in GGM applications such as thickening agents or in 3D printing. The present results allow the design of biorefinery processes to obtain GGM with desirable properties for specific applications.

1. Introduction

Wood is the most abundant source of lignocellulosic biomass on Earth. About 4.8% of the wood biomass produced each year is utilized by humans (Liu et al., 2012). To increase the sustainability of forest industries, it is necessary to develop economic valorization of all lignocellulosic fractions, including hemicelluloses. Galactoglucomannans (GGM) are the main hemicelluloses in softwoods (e.g., spruce), accounting for 14–20% of wood dry mass (Willför et al., 2005). They are branched polysaccharides consisting of glucopyranosyl and mannopyranosyl units in the backbone linked by β-(1 → 4) bonds, and galactopyranosyl units as side groups connected by α-(1→ 6) bonds. The backbone units are partially acetylated at C-2 and C-3 positions with a degree of acetylation of 0.28–0.37 (Willför et al., 2008). GGM can be either recovered from the pulp and paper mill waste-streams (Persson and Jönsson, 2010; Steinmetz et al., 2019; Méndez et al., 2022), or extracted from sawdust, woodchips or wood barks using heat fractionation (Lundqvist et al., 2003), steam explosion (Chadni et al., 2019a), high voltage electrical discharge (Chadni et al., 2019b), and pressurized hot water extraction – PHWE (Song et al., 2008, 2011a, 2011b, 2012). The extracted GGM can replace fossil-based materials in the production of highly value-added products such as hydrocolloids, emulsion stabilizers, and barrier films for many applications in food, pharmaceutical, and cosmetic industries (Kirjoranta et al., 2020; Mikkonen, 2020;

* Corresponding author at: Department of Food and Nutrition, University of Helsinki, P.O. Box 66, FIN-00014 Helsinki, Finland.
E-mail address: kirsi.s.mikkonen@helsinki.fi (K.S. Mikkonen).
[1] Abedalghani Halahlah and Felix Abik contributed equally to this work.

https://doi.org/10.1016/j.indcrop.2023.116656
Received 22 January 2023; Received in revised form 10 March 2023; Accepted 28 March 2023
Available online 7 April 2023

Mikkonen et al., 2010; Valoppi et al., 2019; Willför et al., 2008).

Besides GGM, the spruce extracts contain other components such as lignin and its degradation products, monosaccharides, organic acids, and lipophilic wood extractives (Mänttäri et al., 2015). The total solid content in the PHWE GGM extracts is very low, about 1.8% (w/w) (Al Manasrah et al., 2012). Therefore, further concentration and purification steps such as membrane filtration, to separate GGM from other compounds and concentrate the GGM extracts, are required before the GGM extracts can be further processed into high-value products. However, the fouling taking place during membrane filtration, especially with most commercially available hydrophobic membranes, reduces the permeate production rate and increases the complexity of the membrane filtration operation, consequently increasing the operating cost and reducing GGM yield (Persson and Jönsson, 2010). To reduce the fouling during the membrane filtration of wood hydrolysates, previous studies have focused on the pretreatment of starting materials, membrane selection and modification, and the optimization of processing conditions such as membrane pore size and filtration flow rate and pressure (Al Manasrah et al., 2012; Koivula et al., 2011, 2013, 2015; Mänttäri et al., 2015; Strand, 2016; Thuvander and Jönsson, 2016; Gönder et al., 2011). Wood hydrolysates obtained by PHWE are acidic (pH ≈ 3.3–3.8), and increasing their pH during membrane filtration has been used to reduce membrane fouling. Koivula et al. (2011) found that increasing the pH of birch and spruce hydrolysates from 3.3 to 7–8 markedly reduced the fouling of regenerated cellulose membrane. Similarly, Gönder et al. (2011) observed the significantly reduced membrane fouling at pH 10 compared to pH 4 and pH 7 during nanofiltration of pulp and paper wastewater. The reduced fouling during membrane filtration at high pH is the result of the increased strength of electrostatic repulsion forces between the negatively charged components of the effluent and the negatively charged membrane surface, which inhibits the adsorption of solutes onto the membrane surface. In addition, increasing pH leads to the conversion of some carboxylic acids to salts, decreasing their ability to form hydrogen bonds with the lignin; and the increase of the solubility of numerous colloidal materials such as phenolic compounds, thereby increasing their filterability and decreasing their adhesion to the membrane surface (Bokhary et al., 2018).

Process water from the forest industry and/or wood hydrolysates typically have a high temperature, thus membrane filtration is typically also operated at high temperatures. However, membrane fouling was found to be more severe at higher temperatures than that at lower temperatures. Filtration at higher temperatures increases the amount of solutes that can easily pass, resulting in plugging within the expanded pores and membrane surface (Al-Rudainy et al., 2017; Gönder et al., 2011). Alkaline conditions combined with high temperatures can induce structural changes, like removal of acetyl groups and the hydrolysis of glycosidic bonds in GGM (Al Manasrah et al., 2012; Garrote et al., 2001; Mänttäri et al., 2015; Willför et al., 2008). These changes significantly affect the molar mass and physicochemical properties of GGM (e.g., mechanical properties, solubility, and viscosity), and consequently their functionality and applicability (Hannuksela et al., 2004). For example, the removal of acetyl groups can lead to reduction in GGM solubility and increase their elastic characters. This may also allow for polymer coils to interact with each other and form entanglements or to form stronger interactions with other polymers (Xu et al., 2008).

Despite the importance of the concentration step after extraction, a systematic investigation of the effects of ultrafiltration pH and temperature on characteristics of recovered GGM is lacking. The present work aimed to study the effects of ultrafiltration conditions on the composition and physiochemical properties of GGM powders. GGM was first extracted from sawdust by using PWHE (Kilpeläinen et al., 2014). The extracted GGM liquor was then concentrated by membrane ultrafiltration at three levels of pH (6, 8 and 10) and temperatures (30, 45 and 60 °C), and the ultrafiltrated GGM were spray-dried to obtain powders. The characterization results were compared to those of GGM powders produced by freeze drying and by ethanol precipitation. The results will help wood biorefinery companies in tailoring their recovery processes to obtain GGM with desirable characters for different applications.

2. Materials and methods

2.1. Materials

Spruce sawdust was extracted with a pressurized hot water flow-through system (Kilpeläinen et al., 2014) to obtain GGM. Spruce sawdust was collected from Versowood sawmill in Riihimäki, Finland on September 1, 2021. After collection, sawdust was stored at − 20 °C before extraction. A sample of 92.2 kg of fresh sawdust (39.3 kg of dry mass) was added into a 300 L reactor. After addition, sawdust was first pre-steamed for 10 min with 1.05 kg of 172 °C steam. Sawdust was then extracted at 170 °C with 20 L/min continuous flow for whole 60 min extraction time. The pressure during the extraction was 13.5 bar. The extract (1042 kg) was collected into an intermediate bulk container (IBC) and the pH of the extract was 3.8. Extract's total dissolved solids (TDS) was 0.97% (w/w), indicating 25.7% (w/w) of sawdust was extracted.

Sodium hydroxide (NaOH) used to adjust the pH of GGM extract liquors was obtained from Merk (Darmstadt, Germany). Ethanol (≥ 99.5%, Altia, Helsinki, Finland) was used to produce eGGM via anti-solvent precipitation from spray-dried GGM powders. All chemicals used to characterize GGM powders including Folin-Ciocalteu reagents, methanol, sodium carbonate, L-cysteine, sulfuric acid, dimethyl sulfoxide (DMSO), pullulan, gallic acid, sodium monochloroacetate, lithium bromide (LiBr), trimethylchlorosilane (TMCS), bis(trimethylsilyl)trifluoroacetamide (BSTFA), acetyl chloride, acetyl bromide, acetic acid, perchloric acid, hydrochloric acid (HCl), *n*-heptane, isopropanol and pyridine. Standards for sugar analysis include L-arabinose, D-mannose, D-galactose, D-glucose, D-xylose and D-sorbitol were obtained from Sigma-Aldrich (St Louis, United States). L-Rhamnose monohydrate was obtained from Fluka Biochemika (Buchs, Switzerland). Solutions of Ultrasil™ 75 (pH 2), 110 (pH 10) and 69 (pH 11) used to clean the membrane were obtained from Ecolab (Minnesota, United States). Milli-Q water was used as a solvent for all the experiments.

2.2. Preparation of GGM powders at different ultrafiltration conditions

2.2.1. Ultrafiltrated GGM powders

Ultrafiltration experiments were carried out by an Alfa Laval Labstak® M20 membrane filtration unit (Alfa Laval Nordic Ltd, Soborg, Denmark) using several sets of four Alfa Laval polyethersulfone GR82PP flat sheet ultrafiltration-membranes (0.018 m^2) with a molar mass cut-off 5 kDa.

The unit consisted of a frequency converter attached to a gear pump, feed tank equipped with a heating jacket for automatic temperature control, and a membrane stack consisting of support and spacer plates. The outlet pressure was controlled manually by adjusting a pressure valve. The 7 L aliquots of GGM extract liquors at pH levels of 6, 8 and 10 (adjusted by using 10 M NaOH) was pumped from a feed tank in which the sample was heated to either 30, 45 and 60 °C, to the membrane module by gear pump that applied trans-membrane pressure in the system. During the filtration experiments, the pressure was maintained manually in the system at around 9 bars.

Before use, the membranes were washed in 7 cycles with water and all three Ultrasil™ solutions to activate the membrane. The same approach was used to wash the membrane after filtration was completed. The same set of membranes was used for several ultrafiltration experiments with cleaning by pure water in-between the experiments; however, a new set is used as necessary when the fouling on membrane was not removable by simple cleaning, as evaluated by physical observation of the membranes condition and comparison of pure water flux rate before and after each experiment. Pure water flux measurements were carried out before and after each filtration of the

GGM extract liquor to detect fouling of the membranes. The concentrate was recycled to the feed tank, and the permeate was collected in a separate vessel and measured in order to determine the permeate flow, and hence, to assess the fouling of the membranes during the ultrafiltration. After achieving the desired volume reduction, the concentrate was collected and spray-dried.

Ultrafiltrated GGM concentrates were spray-dried at inlet and outlet air drying temperatures of 170 and 70 °C, respectively (B-290, Buchi Labortechnik GmbHDE, Essen, Germany). The instrument was equipped with two-fluid spray nozzle (0.7 mm in diameter). Compressed air pressure for the nozzle was 6 bar, and its flow rate was 473 L/h. The samples were fed into the drying chamber via a peristaltic pump at a flow rate of 10–15 mL/min. The aspirator was fixed at 90% which corresponds to the flow rate of drying air at 35 m^3/h.

2.2.2. Freeze-dried GGM powders

The GGM extraction liquor was directly freeze-dried (Alpha 2–4 LD plus, Martin Christ, Germany) for 48 h, and then manually ground into the powders.

2.2.3. Ethanol precipitated GGM powders

The GGM powders produced by spray drying of the extracted GGM liquors (without ultrafiltration) were subjected to ethanol-precipitation according to the method reported by Song et al. (2013). In brief, aqueous solutions of GGM (30% w/w) was added to ethanol (1:8 v/v) and left to precipitate overnight. The supernatants were then decanted, and the precipitates were filtered and washed with ethanol, and finally vacuum oven-dried.

Table 1 shows a summary of the sample codes of all GGM powders and their production conditions.

2.3. Characterization of GGM powders

2.3.1. Carbohydrate analysis

The GGM powders were analyzed for their carbohydrate compositions by the standard acid methanolysis method with minor modifications (Laine et al., 2002; Sundberg et al., 1996). Briefly, 10 mg of each GGM sample were methanolyzed in 2 mL of the methanolysis reagent (2 M HCl in dry methanol) at 100 °C for 3 h, worked up by adding 100 μL pyridine, and diluted to 10 mL in methanol. 600 μL aliquots were then silylated at room temperature overnight by TMCS:BSTFA 1:99 (v/v) mixture. After dissolution in 1 mL n-heptane, 1 μL sample was injected into a gas chromatograph fitted with a flame ionization detector (GC-FID) (HP 6890 N, Agilent Technologies, Waldbronn, Germany) fitted with a DB-1 column (30 m in length, 0.25 mm in internal diameter, 0.25 μm of film thickness), and eluted at 20:1 split ratio. The temperature program was as follows: 150 °C (3 min) → 186 °C (2 °C/min) → 200 °C (1 °C/min) → 300 °C (20 °C/min) and at 300 °C (1 min). The relative amount of arabinose, rhamnose, xylose, glucose, galactose, and galacturonic acid were quantified from the flame ionization detector signals using standard curves constructed for each monosaccharide and sorbitol as an internal standard. The amount of monosaccharides was corrected for dehydration (0.88 for pentoses, and 0.9 for hexoses). All GGM samples were prepared in triplicates and each replicate was analyzed once by GC-FID.

Table 1
The sample codes of all investigated GGM samples and their production conditions.

Sample codes	Production conditions
fGGM	Freeze-dried GGM liquor
eGGM	Ethanol-fractionated spray-dried GGM powder
GGM-6/30	Spray drying of GGM extract ultrafiltrated at pH 6/30 °C
GGM-10/30	Spray drying of GGM extract ultrafiltrated at pH 10/30 °C
GGM-6/60	Spray drying of GGM extract ultrafiltrated at pH 6/60 °C
GGM-10/60	Spray drying of GGM extract ultrafiltrated at pH 10/60 °C
GGM-8/45	Spray drying of GGM extract ultrafiltrated at pH 8/45 °C

2.3.2. Degree of acetylation

The degree of acetylation of the GGM samples were determined by alkali hydrolysis followed by enzyme-based quantification. Sample of 100 mg of GGM sample was hydrolyzed overnight under stirring at room temperature by 10 mL 0.1 M NaOH. The mixture was then neutralized by HCl 0.83 M and diluted to 25 mL by milli-Q water. A 1 mL aliquot was centrifuged at 12,074 *g* for 20 min (1–14 K centrifuge, Sigma Laborzentrifugen GmbH, Osterode, Germany), and 50 μL of the supernatant was processed using the Acetic Acid Kit (K-ACET, Megazyme, Wicklow, Ireland) with separate blanks for each GGM types to compensate for the absorption of lignin impurities at 340 nm. The degree of acetylation (D_A) was calculated using the following equation (Eqs. (1) and (2)) (Xu et al., 2010):

$$D_A = \frac{M_H \times \%_{acetyl}}{(M_{acetyl} \times 100) - (M_{acetyl} - 1) \times \%_{acetyl}} \quad (1)$$

where M_H is the molar mass of anhydrohexose unit (162 g/mol), M_{acetyl} is the molar mass of acetyl unit (CH_3CO, 43 g/mol), and $\%_{acetyl}$ is the acetyl content by weight corrected to the mannose and glucose content as only the backbone is acetylated:

$$\%_{acetyl} = \frac{100}{\%_{Man+Glc}} \times \%_{acetyl,calc} \quad (2)$$

where $\%_{Man+Glc}$ is the combined mannose and glucose content per 100 g sample and $\%_{acetyl,calc}$ is the acetyl content calculated from the measurements.

2.3.3. Molar mass analysis

The molar mass of the GGM powders was estimated by size-exclusion chromatography (SEC) using 0.01 M LiBr in DMSO as the solvent. The SEC measurements were conducted on GPCMax (Viscotek Corp, Houston, USA) with Jordi xStream GPC column (Jordi Labs, Mansfield, USA). The column was kept at 60 °C during the measurements. 2 mg/mL of the samples were dissolved in the solvent, filtered using a 0.45 μm syringe filter (Acrodisc 13 mm minispike wwPTFE, Pall Corp, Michigan, USA), and injected (100 μL) into the column. Each sample was eluted at a flow rate of 0.8 mL/min, and the peaks were detected and analyzed by the refractive index (RI, at 40 °C), ultraviolet (UV, 280 nm) and right-angle light scattering (RALS, 90°, 670 nm) detectors. Weight-average (Mw) and number-average (Mn) molar mass values were estimated by a pullulan calibration curve (342, 5900, 11,800, 22,800, and 113,000 g/mol) using signals from the RI detector.

2.3.4. Lignin content

The lignin content of the GGM powders was determined using the cysteine-assisted sulfuric acid method (Lu et al., 2021) with several modifications. 5–10 mg of the GGM powders were weighed in glass reaction vials and mixed with 1 mL of the stock cysteine solution (0.1 g/mL L-cysteine dissolved in 72% sulfuric acid). The mixture was then stirred at room temperature for 1 h, after which the content was transferred to a 50 mL volumetric flask and diluted with Milli-Q water. 5 mL aliquot of the sample was then further diluted to 10 mL in a volumetric flask with Milli-Q water, and the absorbance was measured against a reaction blank (i.e., sample-free reagent that was diluted in the same regime as the samples) using a UV-spectrophotometer at 283 nm (Shimadzu UV-1800, Shimadzu Corp., Kyoto, Japan). The lignin content was determined by extrapolating the absorbance value to a calibration curve of lignin standard and corrected by the recovery rate of a standard lignin sample.

2.3.5. Total phenolic content

The total phenolic content (TPC) of GGM powders was determined using the Folin-Ciocalteu method (Halahlah et al., 2023). In brief,

0.02 mL of sample and 0.78 mL of deionized water were mixed with 0.05 mL of Folin-Ciocalteu reagent. After exactly one minute, 0.15 mL of 20% sodium carbonate was added, and the mixture was allowed to react in the dark for 60 min at room temperature. Total polyphenol content was determined by constructing a calibration curve using gallic acid as a standard at concentrations ranging from 0.05 to 0.5 mg/mL ($R^2 = 0.99$) and measuring sample absorbances at 750 nm with a UV-Vis spectrophotometer (Shimadzu UV-1800, Shimadzu Corp., Kyoto, Japan). The results were presented in mg of gallic acid equivalent (GAE) per g of powder.

2.3.6. Pyrolysis gas chromatography mass spectrometry (Py-GC-MS)

The lignin content and the composition of monolignols were evaluated using EGA/PY-3030D Multi-functional Pyrolyzer (Frontier Laboratories Ltd, Japan) connected to a GCMS-QP2010 SE GC-MS (Shimadzu, Japan). The equipment details and settings, which were applied with slight modifications, have been described earlier (Kynkäänniemi et al., 2022) in addition to the suitability of the analysis method for GGM powders (Lahtinen et al., 2019). The sample size used was 120–150 μg, which was weighed directly in the 80 μL analysis cup. The pyrolysis was performed at 580 °C for a duration of 12 s. The injection was performed using a split mode and a ratio of 1:25. The GC separation was performed as described before (Kynkäänniemi et al., 2022). The pyrolysis products were identified based on the National Institute of Standards and Technology (NIST) database. Chromatograms were processed using the GCMSsolution software (Shimadzu, Japan), which was used to integrate 70 peaks for each chromatogram. The evaluated amount of lignin was based on the areas of guaiacol derivatives (i.e., guaiacyl units).

2.3.7. ζ-potential

The ζ-potential of GGM powders was determined by the dynamic light scattering technique using a Zetasizer Nano-ZS Zen 3600 (Malvern Instruments Ltd., Worcestershire, UK) equipped with a laser (4 mW, 632.8 nm) and backscatter detection at 173° to minimize the influence of multiple scattering. Folded capillary cells DTS1070 (Malvern Panalytical Ltd., Malvern, UK) were used at 25 °C. Each sample were measured at least three times, with 15 − 30 runs per measurement. Aqueous solutions (10% w/w) of GGM powders were prepared by magnetic stirring (600 rpm) and left for stirring overnight (~15 h) at room temperature (22 °C) to achieve maximum dissolution. GGM solutions were diluted by 1000 times in Milli-Q before measurements.

2.3.8. Ultrasonication

Aqueous solutions of GGM (10%, w/v) were ultrasonicated utilizing a Branson 450 W digital sonifier (Branson, Danbury, CT, USA). The instrument operated at a constant frequency of 20 kHz and was equipped with a cylindrical titanium alloy probe (12.70 mm in diameter) that was immersed to the same depth within the solution vials. The experiments were conducted at an amplitude level of 30% for 5 min and these parameters were chosen based on preliminary experiments (Halahlah et al., 2022). To maintain a stable temperature during ultrasonication, the samples were immersed in an ice bath. The possible gelation of GGM samples were visually observed and monitored over one week at room temperature.

2.3.9. Scanning electron microscopy

Morphology of GGM powders was determined using field emission scanning electron microscope (FESEM, S-4800, Hitachi, Tokyo, Japan). The powders were fixed on the double carbon tape which was pre-attached on the metallic specimens (stubs). The fixed samples were then coated with gold/palladium at a thickness of 4 nm for two cycles using a high resolution sputter coater (208HR, Cressington Scientific Instruments, Watford, UK). The coated samples were observed under FESEM at an accelerating voltage of 10 kV, an emission current of 10 μA, a working distance of 10 mm, and magnification of 1000X.

2.3.10. X-ray diffraction

Structure of GGM powders was evaluated by X-ray powder diffraction (XRPD) using Empyrean Alpha 1 X-ray diffractometer (Malvern Panalytical, Malvern Worcestershire, UK). The samples were packed into plastic sample holders and wrapped by kapton tape (Elgood Ltd., Vantaa, Finland). The measurements were performed using copper radiation ($\lambda K\alpha_1 = 1.541$ Å) at a current of 40 mA, voltage of 45 kV, and an angular range of $2\theta = 3–70°$ with step size of 0.01° per second.

2.3.11. Differential scanning calorimetry (DSC)

The thermal properties of GGM powders were determined using a differential scanning calorimeter (DSC-30, Mettler-Toledo, Greifensee, Switzerland). An approximately 8–10 mg sample was weighed in a 40-μL aluminium pan, hermetically sealed, and scanned from 25° to 200°C at a heating rate of 5 °C/min. To prevent water condensation, the measurement cell was flushed with flowing nitrogen gas. Determinations of baseline changes in the heat flow signal, associated with glass transition temperature (T_g), were characterized by the onset and peak temperatures. The melting temperature was determined by the prominent endothermic peaks (T_m). The experiments were carried out in triplicate.

2.4. Experimental design and data analyses

One-way ANOVA accompanied by post-hoc Tukey's test was conducted to distinguish the differences in the mean values of the results from different treatments. The data were evaluated for the normal distribution by analyzing the residuals. The analysis was carried out with JMP™Pro 13 (SAS Institute, Cary, USA) at a 95% confidence level.

To study the effects of ultrafiltration pH (6, 8, and 10) and temperatures (30, 45, and 60 °C) on properties of spruce GGM powders, a 2^2 experimental design added with one central point was employed, totalling five assays run in triplicate in a random order to avoid carry-over effects. Response surface methodology was used to analyze triplicate data to generate second-order multiple regression models (Eq. (3)) for each response variable (x_1 = pH; x_2 = temperature):

$$E(y) = \beta_0 + \beta_1 x_1 + \beta_2 x_2 + \beta_3 x_1 x_2 \quad (3)$$

Regression coefficients were regarded as significant when $p < 0.10$ and the fitting of the models was assessed through the coefficient of determination (R^2) and by the adjusted R^2 values, as outlined elsewhere (Willemann et al., 2020) and the ± 95% confidence intervals for the regression coefficients were calculated using the TIBCO Statistical v. 13.3 (TIBCO Ltd, Tulsa, OK, USA) software.

3. Results and discussion

Ultrafiltration of GGM liquor was conducted at varied combinations of pH and temperature. Membrane fouling was observed by the gradual reduction in rate of flux over a short time after commencing the process and by visually observing the membrane after the process was completed. Membrane fouling was more apparent at high temperature (60 °C). Severe membrane fouling occurred at 60 °C, when combined with a high pH (10), leading to membrane compression which resulted in a highly reduced permeate rate and an increase in the time and complexity of the membrane filtration operation. However, 4–6 L of permeate was still successfully separated at all conditions, and 1–2 L of retentate was collected for spray drying and further analysis.

3.1. Carbohydrate composition

Chemical analyses were conducted to determine the effect of membrane filtration conditions on the structure of the recovered GGM. As indicated in Table 2, the carbohydrate composition of GGM powders ultrafiltrated at various conditions of pH and temperature were not significantly different from each other ($p > 0.05$). Mannose, glucose, and

Table 2
Carbohydrate composition (g/100 g powder, average value ± standard error), weight-average molar mass and dispersity of GGM powders. Refer to Table 1 for sample codes.

Samples	Arabinose	Rhamnose	Xylose	Mannose	Galactose	Glucose	Weight-average molar mass (Mw, Da)	Dispersity (Mw/Mn)
fGGM	5.6 ± 0.3^{c}	0.3 ± 0.4^{b}	13.6 ± 0.4^{c}	$44.5 \pm 1.2a^{ab}$	8.4 ± 0.2^{bc}	12.5 ± 0.2^{b}	3200	2.8
eGGM	0.3 ± 0.2^{d}	0.4 ± 0.3^{a}	12.3 ± 0.3^{bc}	59.3 ± 1.3^{c}	9.3 ± 0.2^{b}	16.8 ± 0.4^{c}	4300	2.6
GGM-6/30	2.1 ± 0.2^{a}	n.d.	10.9 ± 0.1^{ab}	44.0 ± 2.5^{ab}	7.6 ± 0.3^{c}	12.4 ± 0.7^{ab}	3400	2.8
GGM-10/30	2.0 ± 0.0^{a}	n.d.	10.2 ± 0.2^{a}	42.7 ± 0.7^{ab}	7.2 ± 0.2^{ac}	12.0 ± 0.3^{ab}	3400	2.7
GGM-6/60	3.0 ± 0.4^{b}	n.d.	10.3 ± 0.4^{a}	36.4 ± 0.5^{a}	6.8 ± 0.2^{ac}	10.4 ± 0.2^{ab}	3700	2.5
GGM-10/60	1.9 ± 0.3^{ab}	n.d.	10.2 ± 1.2^{a}	42.1 ± 5.1^{a}	7.0 ± 0.8^{ac}	11.9 ± 1.5^{ab}	2200	2.2
GGM-8/45	2.0 ± 0.1^{a}	0.4 ± 0.3^{a}	11.2 ± 0.2^{a}	44.9 ± 3.1^{a}	7.6 ± 0.4^{ac}	12.6 ± 0.6^{ab}	3200	2.7

n.d. = not detected. Sample means with different letters in the same column are significantly different ($p < 0.05$).

galactose were the dominating monosaccharides, confirming that the fractions collected were composed primarily of GGM. The presence of xylose and arabinose suggested that arabinoxylans, the second most abundant hemicelluloses in spruce wood, were co-extracted along with GGM. Ultrafiltration appeared to have significantly reduced the amount of xylose and arabinose as compared to those of fGGM. This was consistent with the findings of Song et al. (2013), who performed sequential membrane filtration of GGM using membranes with progressively smaller molar mass cut-off values. They found that the arabinose and xylose content of the retained polysaccharides increased as the filtration progressed to membranes with lower molar mass cut-off values. This indicates that the arabinoxylan fraction tend to be shorter than the GGM itself and thus will pass more easily through the membrane instead of being retained. The general increase in xylose, mannose, galactose, and glucose content per 100 g mass of the extract in eGGM could be attributed to the more concentrated polysaccharide content following partial lignin removal, as the same amount of extract would have more polysaccharide and less lignin after precipitation. In comparison, Thuvander and Jönsson (2016) found that the monosaccharide composition in the retentate during ultrafiltration of TMP GGM is dependent on the type of membrane, and the presence of large components such as suspended solids and colloidal extractives prevent the separation of GGM from low molar mass monosaccharides.

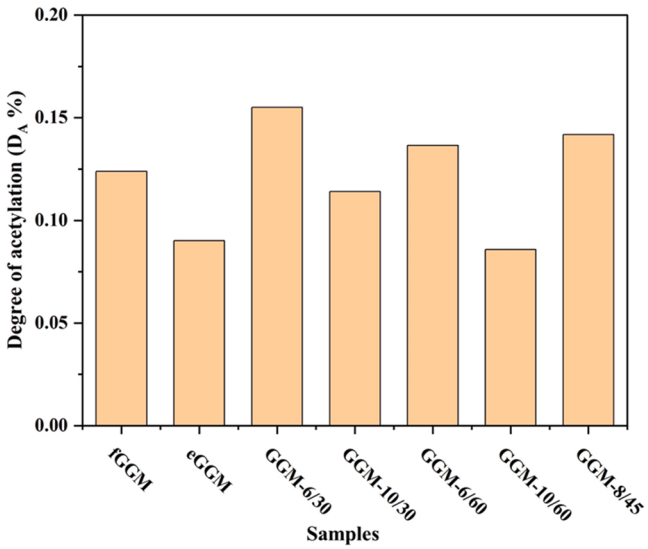

Fig. 1. Degree of acetylation of GGM powders. Refer to Table 1 for sample codes.

3.2. Degree of acetylation

Native GGM is acetylated and contains acetyl groups in every second mannose unit with the D_A of 15–20% (Lahtinen et al., 2019). A portion of the acetyl groups are removed during PHWE process to the extent dictated by the duration and extraction temperature (Song et al., 2008), which suggested that the conditions of any post-extraction treatments might also influence the D_A. The acetylation is susceptible to hydrolysis in alkali condition (Li et al., 2014; Wang et al., 2011). As shown in Fig. 1, among ultrafiltrated GGM samples, GGM-10/60 samples had the lowest D_A, followed by GGM-10/30 samples. Both GGM-10/60 and GGM-10/30 samples had lower D_A values than fGGM samples while the other ultrafiltrated GGM samples had higher D_A values than fGGM samples. These results indicated that ultrafiltration at high pH induced the deacetylation of GGM, which was accelerated by higher temperature. The eGGM powders had similar D_A to that of GGM-10/60; the fraction with a higher D_A might have associated more with the ethanol-soluble fraction and hence was removed during precipitation process.

3.3. Molar mass

Molar mass was determined to evaluate the effect of membrane filtration conditions to the size of the recovered GGM. As shown in Table 2, GGM-10/60 powders had a molar mass of 2200 Da, which was lower than that of the other ultrafiltrated GGM samples (3200–3700 Da). Ultrafiltration at pH 10 and 60 °C possibly induced the degradation of GGM molecules due to harsh conditions. Xu et al. (2007) reported that increasing the temperature above 37 °C can cause a degradation of GGM structure, and the molar mass of GGM decreased considerably with treatment time at temperatures above 60 °C. The ultrafiltrated GGM powders other than GGM-10/60 had the molar mass similar to that of fGGM powders, but smaller than that of eGGM powders. The molar mass distribution of PHWE GGM is known to be highly disperse as reflected from the dispersity value (Table 2) and the SEC chromatograms (Fig. S1); however, the fraction with a higher molar mass is insoluble in ethanol, thereby shifting the average molar mass value of the ethanol precipitated fraction to a higher value (Carvalho et al., 2020). This trend was not only observed for PHWE GGM but also for TMP GGM (Zasadowski et al., 2014; Xu et al., 2007).

3.4. Total phenolic and lignin content

In addition to GGM, the PHWE spruce extracts contain residual phenolic compounds, mainly lignin, that may significantly contribute to the functionality of the concentrated extracts (Lahtinen et al., 2019). The results of the two complementary analyses, TPC and lignin content, were in good agreement (Fig. 2). The ultrafiltrated GGM powders had TPC in the range of 54–63 mg GAE/g, which is similar to that of spray-dried GGM powders reported by Mikkonen et al. (2019). Meanwhile, their lignin content was between 14 and 16 mg/100 mg powder, which is also similar to previously reported values (Ho et al., 2022). These values are significantly lower than that of fGGM powders, suggesting that ultrafiltration removed portions of phenolic compounds, and the removal was slightly enhanced by increasing ultrafiltration temperature. However, the variations between the ultrafiltrated GGM samples were not significantly different ($p > 0.05$). According to Al-Rudainy et al. (2017), the high retention of GGM and lignins (phenolic compounds) in the ultrafiltration might have resulted from the

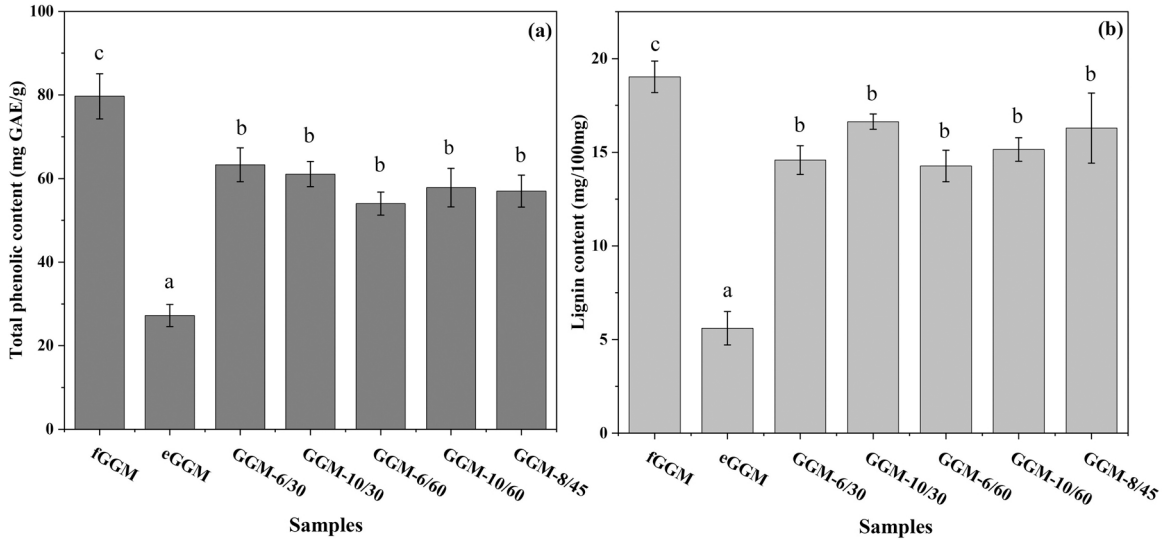

Fig. 2. Total phenolic content (a), and lignin content (b) of GGM powders. The data are shown in means ± standard error (n = 3) and means with different letters in the same graph indicate significant differences at $p < 0.05$. Refer to Table 1 for sample codes.

formation of a cake/gel layer on the membrane and not by the membrane itself. Such layer can cause compaction of the membrane which can lead to lower the flux through the membrane. This can explain for the lower TPC of ultrafiltrated GGM samples as compared to fGGM samples (79 mg GAE/g). eGGM samples had the lowest TPC (27 mg GAE/g) and lignin content (5.6 mg/100 mg powder), as ethanol precipitation removes part of the lignin and thus phenolic compounds (Mikkonen et al., 2019).

3.5. Py-GC-MS

We have earlier found that Py-GC-MS is a practical semiquantitative method for the estimation of lignin content and composition in hemicellulose materials (Lahtinen et al., 2019). When comparing the total amount of guaiacyl units (G-units, i.e., methoxyphenol), Lignin-G-tot, which was used to estimate the content of lignin, the amount was on a similar magnitude with lignin content obtained from cysteine-assisted sulfuric acid (CASA) method (Lu et al., 2021) (Table 3). The CASA method, on the other hand, correlates with the Klason method, giving further evidence that Py-GC-MS is useful for the semiquantitative analysis of lignin residues in polysaccharides. For a more reliable result, the other aromatic fragments, which can originate from carbohydrates, were not taken into account (Bausch et al., 2021). When considering each produced fragments separately, the amount of guaiacol varied between the different samples. There seemed to be a linear correlation between the ultrafiltration pH and the amount of guaiacol ($R^2 = 0.959$, n = 5). This result indicated some differences in the chemical structures of lignins between the ultrafiltrated samples. However, further investigations such as nuclear magnetic resonance spectroscopy are required to understand these differences in detail.

Table 3
Py-GC/MS analysis of GGM powders. The results are presented as peak areas (%) of all various G-units and their sums for each sample.

Samples	Lignin-G-tot	Guaiacol	2-Methoxy-4-vinylphenol	Creosol	Vanillin
Retention times (min)		7.57	10.89	9.13	12.09
fGGM	26.36	2.18	2.70	1.79	2.08
eGGM	2.64	0.56	0.73		
GGM-6/30	18.06	3.72	2.21	1.49	1.11
GGM-10/30	19.25	4.83	2.21	1.49	1.53
GGM-6/60	20.59	3.46	2.60	1.72	1.66
GGM-10/60	18.85	5.05	2.54	1.09	1.42
GGM-8/45	19.31	4.42	2.10	1.84	1.16

3.6. ζ-potential

The ζ-potential of GGM samples was determined to evaluate their colloidal properties. As indicated in Fig. 3, the ζ-potential values of all investigated GGM powders were negative. The sources of charges could be uronic acid residues and coextracted phenolic compounds linked naturally to GGM (Bhattarai et al., 2020). As uronic acid residues were not detected in quantifiable amounts in our analysis, the variations of ζ-potential is more likely to have resulted from the changes occurring to the co-extracted phenolic residues. Given that the lignin analysis showed non-significant differences of the lignin content for ultrafiltrated GGM powders (Fig. 2a), variations might have arisen due to the altered molecular structure of the lignin residues, which may have been caused by the different ultrafiltration conditions. This hypothesis is supported by

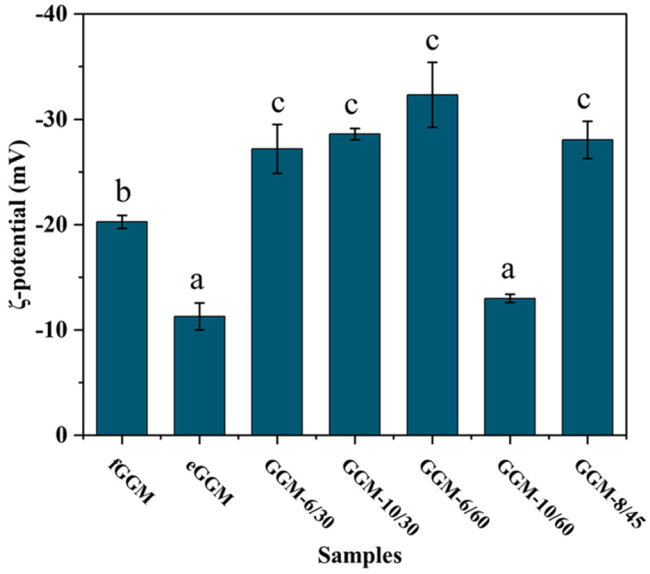

Fig. 3. ζ-potential of GGM powders. The data are shown in means ± standard errors (n = 3) and means with different letters indicate significant differences at $p < 0.05$. Refer to Table 1 for sample codes.

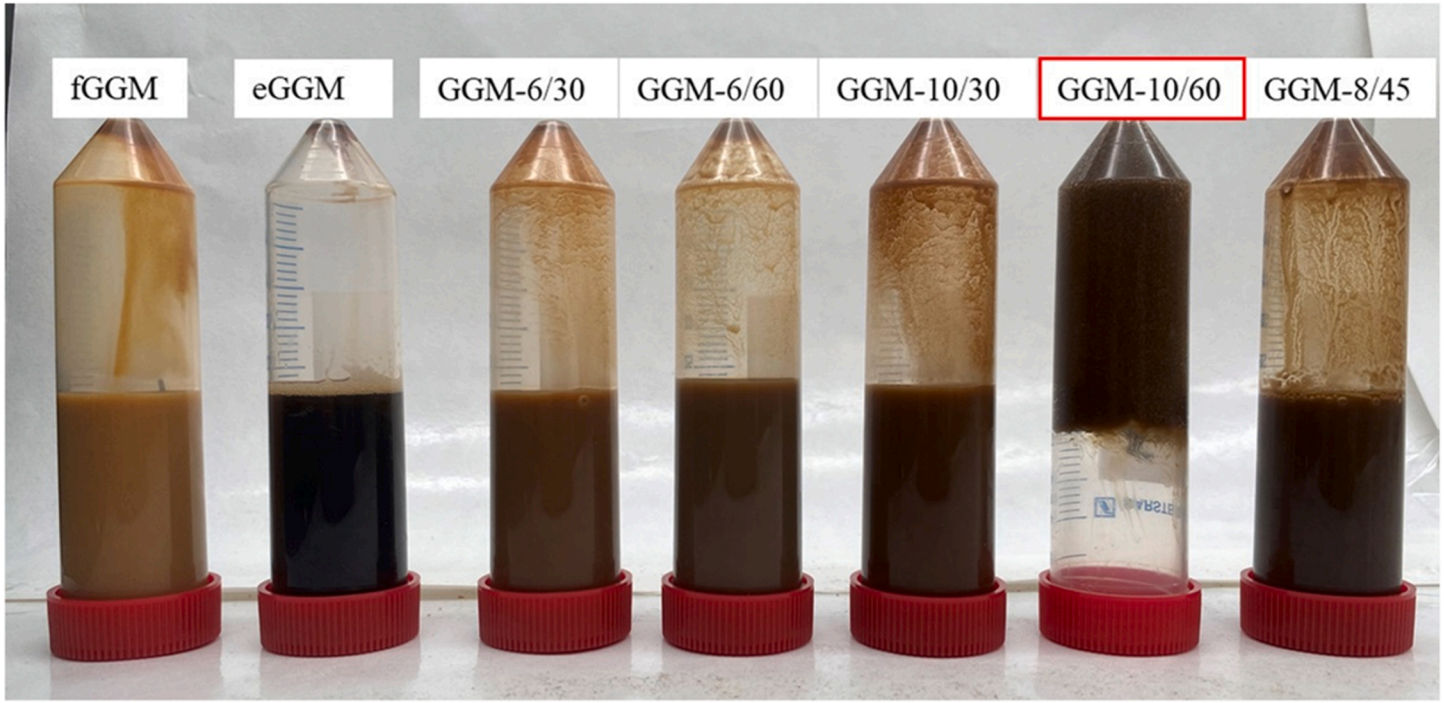

Fig. 4. Photos illustrating the gelation of GGM-10/60 samples after 2 h of ultrasonication and non-gelation of the other ultrasonicated GGM samples over 1 week of storage at room temperature.

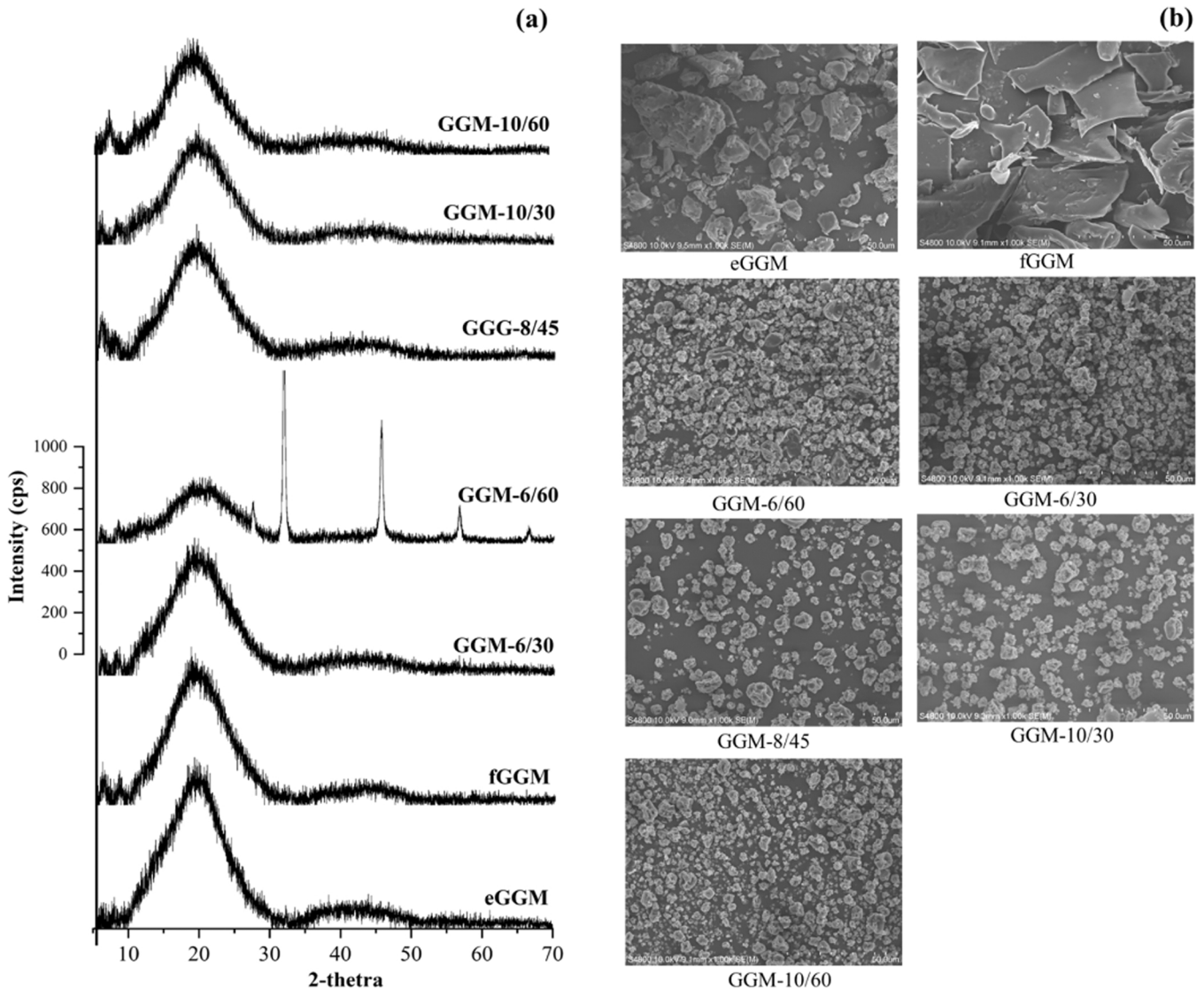

Fig. 5. X-ray diffraction (a) and scanning electron microscopy (b) of GGM powders. Refer to Table 1 for sample codes.

the differences in Py-GC-MS analysis, where differences in formed guaiacol might have arisen during the degradation process (Table 3). Furthermore, differences in the degree of acetylation could have altered the folding behavior of the GGM, altering the charge distribution on the surface of GGM particles in the different samples. GGM-10/60 samples had significantly lower absolute ζ-potential (13 mV) than that of the other ultrafiltrated samples (23–33 mV) ($p < 0.05$). This value is similar to that of eGGM despite their significant differences in the content of lignin and phenolic compounds (Fig. 2).

3.7. Effect of ultrasonication

The GGM solutions were treated by ultrasonication to alter their solubility and monitor possible changes in their consistency. After ultrasonication, gel formation from GGM-10/60 was visually observed after 2 h, while the other GGM samples did not form gels even after being stored for over a week at room temperature after the sonication treatment (Fig. 4). This is the first time that gelation has been observed for PHWE GGM, and also quite unique given the low average molar mass value of PHWE GGM compared to TMP GGM. As such, this observation might indicate an enhanced intermolecular interaction that was not observed previously for PHWE GGM, which could have arisen from a number of factors. Firstly, GGM-10/60 had the lowest D_A compared to the other samples. It has been previously discovered that the viscosity of deacetylated TMP GGM solutions was higher than that of the acetylated ones due to the intermolecular associations occurring after the removal of acetyl groups (Xu et al., 2007). Similarly, acetyl groups were found to be the main hindrance of the GGM molecules from becoming close to each other and forming packing lattice (Xu et al., 2008). It was therefore plausible that the lack of acetylation enhances the intermolecular interaction between the GGM molecules to the point of gelation. Secondly, the low absolute ζ-potential value of GGM-10/60 indicated a weaker electrostatic repulsion among the different GGM samples, which could lead to higher degree of agglomeration (Vallar et al., 1999). However, eGGM did not undergo gelation despite having similar DA and ζ-potential values, which indicate that the lignin content is also crucial in the gelation. Therefore, we propose that the combination of low DA, low ζ-potential value, and high lignin content is the major driving force behind the gelation process.

Additionally, we also noticed that a high-energy treatment of the GGM solutions is necessary in order to trigger the gelation process, as a simple overnight stirring did not cause the samples to gel. Previous studies on PHWE GGM indicated a higher viscosity at 12% (w/w) and the formation of shear-sensitive colloidal aggregates over time, implying that PHWE GGM has the natural tendency to associate even without forming gels (Mikkonen et al., 2016; Bhattarai et al., 2020). We

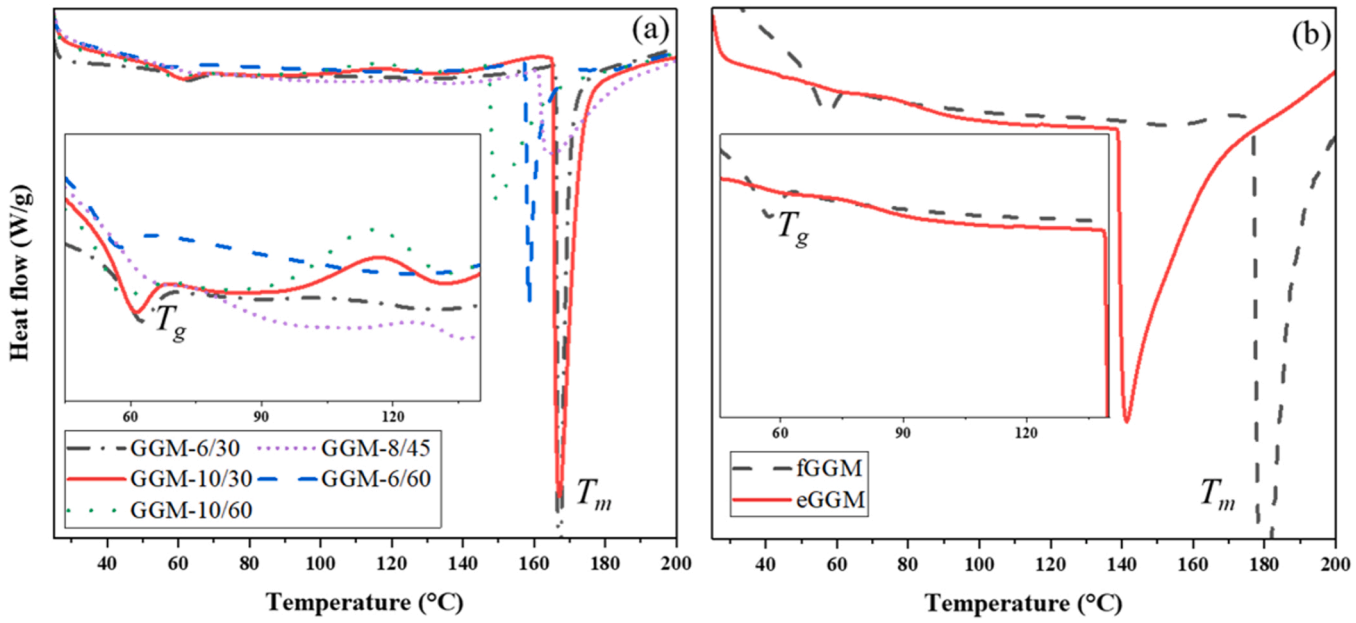

Fig. 6. DSC curves of ultrafiltrated GGM powders (a), and eGGM and fGGM powders (b). The small graphs representing the resolution of the original graphs in a range of 45–140 °C, T_g: glass transition temperature, T_m: melting temperature. Refer to Table 1 for sample codes.

therefore hypothesize that the shear forces generated by cavitation bubbles formed during ultrasonication facilitated the gel formation by breaking the GGM aggregates in the solution, which then enabled the fragments to re-aggregate in a different manner and form a gel network. It is well known that the cavitation bubbles generated by ultrasonication can produce shear forces powerful enough to break covalent bonds (Amiri et al., 2018). Nevertheless, this hypothesis requires further characterization of the GGM solution before and after gelation to further clarify the gelation mechanism. Particularly, understanding the supramolecular structure of PHWE GGM before and after gelation, as well as whether the gelation involves the formation of new covalent bonds that act as intermolecular bridges between the GGM molecules.

3.8. X-ray diffraction and scanning electron microscopy

Morphological characterization of GGM powders was made to evaluate the physical properties of the powders. As indicated in Fig. 5(a), GGM-6/60 had some degree of crystallinity with two main sharp peaks at $2\theta = 31.6°$ and 45.4° observed on its XRD spectrum while all other GGM samples had amorphous structure as their XRD spectra were only characterized by a broad peak. The crystallinity of GGM-6/60 is possibly due to the effect of lignin on the nucleation growth of crystalline polysaccharide. It was found that the crystallization of polymers was strongly enhanced by the nucleation action of lignin particles (Canetti et al., 2006), suggesting that it is possible for lignin to affect the crystallization process of GGM. However, the lignin content in ultrafiltrated GGM samples was similar and significantly lower than that of fGGM powders (Fig. 2), possibly suggesting effects of ultrafiltration pH and temperature on crystallization behavior of GGM in the presence of lignin. The XRD spectrum of GGM-6/60 is similar to that of alkaline lignin obtained from masson pine sulfate pulping liquor by diluting to 10% (w/w), adjusting pH to 3.0, heating at 50 °C for 1 h and filtrating (Ye et al., 2017).

Morphological features shown by SEM images in Fig. 5(b) showed marked differences among fGGM, eGGM and ultrafiltrated GGM samples. The fGGM powders had a skeletal-like structure with smooth surface; and eGGM powders included particles with cubic, tetragonal and triclinic shapes, and there were many clefts on their surface. All ultrafiltrated GGM powders consisted of spherical or oval shape particles with dented structure, which are typical characteristics of spray dried powders caused by a combination of several factors such as drying rate, atomization mechanism, uneven shrinkage at early stages of drying, and the viscoelastic properties of the materials (Anandharamakrishnan, Ishwarya, 2015). The similarity in the morphology of ultrafiltrated GGM powders is due to the same spray drying conditions. The results indicated that the morphology of GGM powders is determined by the dehydration method instead of ultrafiltration conditions. In addition, by rough estimation from SEM images, all ultrafiltrated GGM samples had a similar particle size, which was much smaller than that of fGGM and eGGM.

3.9. Differential scanning calorimetry

The glass transition temperature (T_g) of powders is an important property since it impacts the powder stability during long-term storage. When amorphous powders are stored at temperatures above their T_g, they become rubbery, increasing molecular mobility and the rate of physicochemical changes such as collapse, caking, agglomeration, browning, and oxidation. As a result, spray-dried powders should be kept at temperatures lower than their T_g (Bhandari and Howes, 1999). DSC curves of all GGM powders presented in Fig. 6 illustrated a major transition at 50–60 °C. This transition is suggested to be linked to T_g of lignin residues (Olsson and Salmén, 1997; Stelte et al., 2011). It is noticed that the reported T_g values of GGM in the literature are somewhat inconclusive, for example 180 °C (Nypelö et al., 2016), 55–65 °C (Hartman et al., 2006), and 43 °C (Xu et al., 2007). This could be because of both variations in the characteristics of wood hemicelluloses affected by extraction methods, and in the experimental procedures. Polymers with the higher molar mass, amounts of bulky and inflexible side groups, degree of cross-linking, and amounts of polar groups have the higher T_g (Roos, 2010). GGM-10/30, GGM-10/60 and GGM-8/45 exhibited another endothermic change at around 120–130 °C which can be explained by either a second T_g or due to water evaporation as was suggested by other researchers (Castro-López et al., 2021; Leena et al., 2020).

A sharp endothermic peak at around 150–180 °C which was observed on the DSC curves of all GGM powders possibly originated from the melting of crystalline proportions (e.g., GGM-6/60) and/or sample decomposition (T_m). Among ultrafiltered GGM samples, GGM-10/60 powders had the lowest T_m value (~150 °C), followed by GGM-

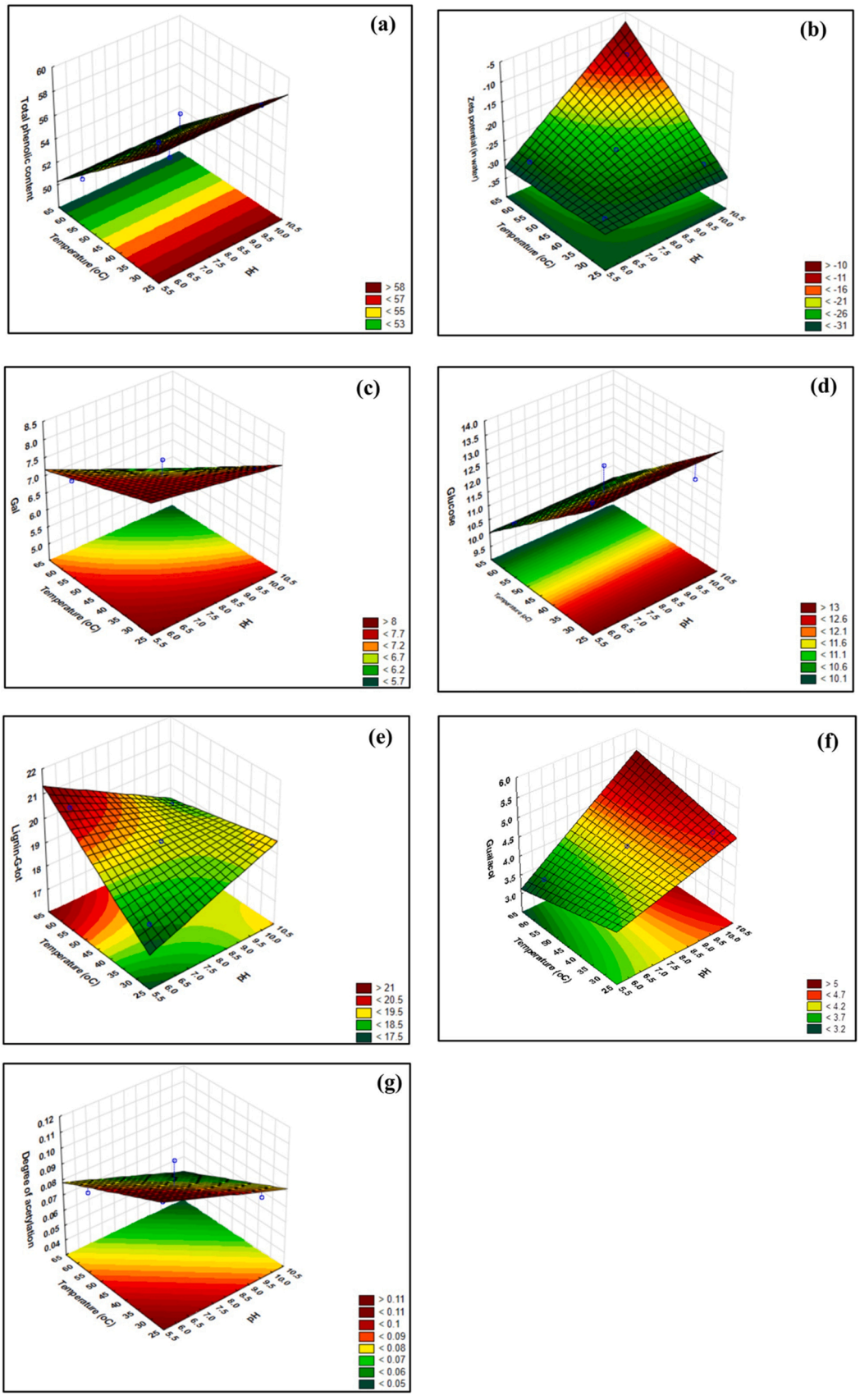

Fig. 7. Effects of temperature and pH on total phenolic content (a), ζ-potential (b), galactose (c), glucose (d), lignin-G-tot (e), guaiacol (f), and degree of acetylation (g).

6/60 powders (~160 °C) while T_m values of the other ultrafiltered GGM samples were above 170 °C. The results indicated the ultrafiltration conditions, especially temperature (60 °C) markedly affected heat stability of GGM powders. It appeared that removal of lignin, phenolic compounds and acetyl groups reduces the heat stability of GGM powders. This could also explain for a lower T_m of eGGM powders (140 °C) as compared to that of fGGM powders (180 °C) (Fig. 6b).

3.10. Modeling the experimental data

Response surface methodology (RSM) is usually applied to experimental data to understand the effects of important factors (e.g., time, temperature and pH) on quality parameters (e.g., chemical composition, physical and sensory properties) of the process and/or product (Bezerra et al., 2008). Trying to understand the effects of ultrafiltration pH and temperature on the properties of GGM powders, RSM was applied, and results can be found in Table S1 (Supplementary materials). The regression models explained accurately the TPC, ζ-potential, galactose, glucose, molar mass, guaiacol, and lignin-G contents. For these responses, the coefficient of determination (R^2) was higher than 0.70, meaning that the RSM models were able to explain more than 70% of the variance in data. In practice, the RSM models shown in Table S1 can be used to predict, with ± 95% confidence, the mean value of each response without performing the actual measurement in the lab. Interestingly, for molar mass, neither the temperature ($p = 0.076$) nor the pH ($p = 0.059$) was significant in increasing the mean molar mass values, but their interaction was significant ($p = 0.048$). Similar trends were observed for lignin-G-tot, guaiacol, and galactose. To facilitate the observation of the effects of temperature and pH on the responses, response surface plots were generated and are presented in Fig. 7.

On the other hand, the RSM models proposed for lignin content, degree of acetylation, arabinose, rhamnose, xylose, mannose, creosol, vanillin, 2-methoxy-4-vinylphenol, dispersity (Mw/Mn) could not be fitted into a polynomial equation. This can be observed by the low R^2 values (<0.70) and by the non-significance ($p > 0.05$) of temperature and/or pH on each response. In practice, the RSM models cannot be used for prediction purposes at the factors' range studied.

4. Conclusion and outlook

This work confirmed that the ultrafiltration parameters including pH and temperature had high impact on the composition and physicochemical properties of GGM powders and can be used to tailor the product properties. High temperature (60 °C) and pH (10) led to membrane fouling and lower flux of the feed, and samples obtained under these conditions had lower molar mass, degree of acetylation and absolute ζ-potential compared to the other samples. Furthermore, total phenolic content and carbohydrate contents decreased as temperature of ultrafiltration increased. Carbohydrate contents of all ultrafiltrated GGM samples (especially arabinose and xylose) were lower than in fGGM as they were released during ultrafiltration. Unlike fGGM and eGGM and the rest of ultrafiltrated samples, GGM-10/60 formed a gel after ultrasonication. This research indicated the necessity of controlling the concentration process of GGM liquor after extraction. Furthermore, GGM with desired physicochemical properties could be produced by adjusting ultrafiltration process conditions. GGM sample which formed gel structure opened new possible applications of GGM powders that could be used as thickening agents or in 3D printing, for examples.

Funding

Academy of Finland (project no. 322514), and Finnish Natural Resources Research Foundation (No: 20210017).

CRediT authorship contribution statement

Abedalghani Halahlah: Conceptualization, Methodology, Investigation, Formal analysis, Writing - original draft. **Felix Abik**: Methodology, Investigation, Formal analysis, Writing - review & editing. **Maarit Lahtinen**: Formal analysis, Writing - review & editing. **Asmo Kemppinen**: Methodology & Investigation. **Kalle Kaipanen**: Formal analysis. **Petri O. Kilpeläinen**: Conceptualization, Methodology, Writing - review & editing. **Daniel Granato**: Statistical analysis, Writing - review & editing. **Thao Minh Ho**: Conceptualization, Supervision, Funding, Methodology, Investigation, Formal analysis, Writing - review & editing. **Kirsi S. Mikkonen**: Conceptualization, Supervision, Funding, Writing - review & editing.

Declaration of Competing Interest

The authors declare that they have no known competing financial interests or personal relationships that could have appeared to influence the work reported in this paper.

Data availability

Data will be made available on request.

Acknowledgment

The authors acknowledge the Academy of Finland (project no. 322514), and Finnish Natural Resources Research Foundation (No: 20210017) for funding, Mr. Troy Faithfull for his proofreading, and Fabio Valoppi for the use of the mini-spray dryer.

Appendix A. Supporting information

Supplementary data associated with this article can be found in the online version at doi:10.1016/j.indcrop.2023.116656.

References

Al Manasrah, M., Kallioinen, M., Ilvesniemi, H., Mänttäri, M., 2012. Recovery of galactoglucomannan from wood hydrolysate using regenerated cellulose ultrafiltration membranes. Bioresour. Technol. 114, 375–381.

Al-Rudainy, B., Galbe, M., Wallberg, O., 2017. Influence of prefiltration on membrane performance during isolation of lignin-carbohydrate complexes from spent sulfite liquor. Sep. Purif. Technol. 187, 380–388.

Amiri, A., Mousakhani-Ganjeh, A., Torbati, S., Ghaffarinejhad, G., Kenari, R.E., 2018. Impact of high-intensity ultrasound duration and intensity on the structural properties of whipped cream. Int. Dairy J. 78, 152–158.

Anandharamakrishnan, C., Ishwarya, S.P., 2015. Encapsulation of bioactive ingredients by spray drying. Spray Drying Techniques for Food Ingredient Encapsulation; Anandharamakrishnan, C., Ishwarya, S.P., Eds. John Wiley & Sons Ltd,, Chicago, IL, USA, pp. 156–179.

Bausch, F., Owusu, D.D., Jusner, P., Rosado, M.J., Rencoret, J., Rosner, S., Del Río, J.C., Rosenau, T., Potthast, A., 2021. Lignin quantification of papyri by TGA—not a good idea. Molecules 26 (*14*), 4384.

Bezerra, M.A., Santelli, R.E., Oliveira, E.P., Villar, L.S., Escaleira, L.A., 2008. Response surface methodology (RSM) as a tool for optimization in analytical chemistry. Talanta 76, 965–977.

Bhandari, B., Howes, T., 1999. Implication of glass transition for the drying and stability of dried foods. J. Food Eng. 40, 71–79.

Bhattarai, M., Valoppi, F., Hirvonen, S.P., Hietala, S., Kilpeläinen, P., Aseyev, V., Mikkonen, K.S., 2020. Time-dependent self-association of spruce galactoglucomannans depends on pH and mechanical shearing. Food Hydrocoll. 102, 105607.

Bokhary, A., Tikka, A., Leitch, M., Liao, B., 2018. Membrane fouling prevention and control strategies in pulp and paper industry applications: A review. J. Membr. Sci. Res. 4, 181–197.

Canetti, M., Bertini, F., De Chirico, A., Audisio, G., 2006. Thermal degradation behaviour of isotactic polypropylene blended with lignin. Polym. Degrad. Stab. 91 (3), 494–498.

Carvalho, D.M.D., Lahtinen, M.H., Lawoko, M., Mikkonen, K.S., 2020. Enrichment and identification of lignin–carbohydrate complexes in softwood extract. ACS Sustain. Chem. Eng. 8 (31), 11795–11804.

Castro-López, C., Espinoza-González, C., Ramos-González, R., Boone-Villa, V.D., Aguilar-González, M.A., Martínez-Ávila, G.C., Aguilar, C.N., Ventura-Sobrevilla, J.M., 2021.

Spray-drying encapsulation of microwave-assisted extracted polyphenols from Moringa oleifera: Influence of tragacanth, locust bean, and carboxymethyl-cellulose formulations. Food Res. Int. 144, 110291.
Chadni, M., Grimi, N., Bals, O., Ziegler-Devin, I., Brosse, N., 2019a. Steam explosion process for the selective extraction of hemicelluloses polymers from spruce sawdust. Ind. Crops Prod. 141, 111757.
Chadni, M., Grimi, N., Ziegler-Devin, I., Brosse, N., Bals, O., 2019b. High voltage electric discharges treatment for high molecular weight hemicelluloses extraction from spruce. Carbohydr. Polym. 222, 115019.
Garrote, G., Dominguez, H., Parajo, J., 2001. Study on the deacetylation of hemicelluloses during the hydrothermal processing of Eucalyptus wood. Holz als Roh-und Werkst. 59, 53–59.
Gönder, Z.B., Arayici, S., Barlas, H., 2011. Advanced treatment of pulp and paper mill wastewater by nanofiltration process: Effects of operating conditions on membrane fouling. Sep. Purif. Technol. 76, 292–302.
Halahlah, A., Piironen, V., Mikkonen, K.S., Ho, T.M., 2022. Wood Hemicelluloses as Innovative Wall Materials for Spray-Dried Microencapsulation of Berry Juice: Part 1—Effect of Homogenization Techniques on their Feed Solution Properties. *Food and Bioprocess*. Technology 1–21.
Halahlah, A., Räikkönen, H., Piironen, V., Valoppi, F., Mikkonen, K.S., Ho, T.M., 2023. Wood hemicelluloses as sustainable wall materials to protect bioactive compounds during spray drying of bilberries. Powder Technol. 415, 118148.
Hannuksela, T., Holmbom, B., Lachenal, D., 2004. Effect of sorbed galactoglucomannans and galactomannans on pulp and paper handsheet properties, especially strength properties. Nord. Pulp Pap. Res. J. 19, 237–244.
Hartman, J., Albertsson, A.C., Lindblad, M.S., Sjöberg, J., 2006. Oxygen barrier materials from renewable sources: Material properties of softwood hemicellulose-based films. J. Appl. Polym. Sci. 100, 2985–2991.
Ho, T.M., Abik, F., Hietala, S., Isaza Ferro, E., Pitkänen, L., Juhl, D.W., Mikkonen, K.S., 2022. Wood lignocellulosic stabilizers: effect of their characteristics on stability and rheological properties of emulsions. Cellulose 30, 753–773.
Kilpeläinen, P., Hautala, S., Byman, O., Tanner, L., Korpinen, R., Lillandt, M.K., Pranovich, A., Kitunen, V., Willför, S., Ilvesniemi, H., 2014. Pressurized hot water flow-through extraction system scale up from the laboratory to the pilot scale. Green. Chem. 16, 3186–3194.
Kirjoranta, S., Knaapila, A., Kilpeläinen, P., Mikkonen, K.S., 2020. Sensory profile of hemicellulose-rich wood extracts in yogurt models. Cellulose 27, 7607–7620.
Koivula, E., Kallioinen, M., Preis, S., Testova, L., Sixta, H., Mänttäri, M., 2011. Evaluation of various pretreatment methods to manage fouling in ultrafiltration of wood hydrolysates. Sep. Purif. Technol. 83, 50–56.
Koivula, E., Kallioinen, M., Sainio, T., Antón, E., Luque, S., Mänttäri, M., 2013. Enhanced membrane filtration of wood hydrolysates for hemicelluloses recovery by pretreatment with polymeric adsorbents. Bioresour. Technol. 143, 275–281.
Koivula, E., Kallioinen, M., Mänttäri, M., Kleen, M., 2015. Activated carbon treatment to improve ultrafiltration performance in recovery of hemicelluloses from wood extracts. Nord. Pulp Pap. Res. J. 30, 207–214.
Kynkäänniemi, E., Lahtinen, M.H., Jian, C., Salonen, A., Hatanpää, T., Mikkonen, K.S., Pajari, A.-M., 2022. Gut microbiota can utilize prebiotic birch glucuronoxylan in production of short-chain fatty acids in rats. Food Funct. 13, 3746–3759.
Lahtinen, M.H., Valoppi, F., Juntti, V., Heikkinen, S., Kilpeläinen, P.O., Maina, N.H., Mikkonen, K.S., 2019. Lignin-rich PHWE hemicellulose extracts responsible for extended emulsion stabilization. Front. Chem. 7, 871.
Laine, C., Tamminen, T., Vikkula, A., Vuorinen, T., 2002. Methylation analysis as a tool for structural analysis of wood polysaccharides. Holzforschung 56, 607–614.
Leena, M.M., Antoniraj, M.G., Moses, J., Anandharamakrishnan, C., 2020. Three fluid nozzle spray drying for co-encapsulation and controlled release of curcumin and resveratrol. J. Drug Deliv. Sci. Technol. 57, 101678.
Li, J., Ye, T., Wu, X., Chen, J., Wang, S., Lin, L., Li, B., 2014. Preparation and characterization of heterogeneous deacetylated konjac glucomannan. Food Hydrocoll. 40, 9–15.
Liu, S., Lu, H., Hu, R., Shupe, A., Lin, L., Liang, B., 2012. A sustainable woody biomass biorefinery. Biotechnol. Adv. 30 (4), 785–810.
Lu, F., Wang, C., Chen, M., Yue, F., Ralph, J., 2021. A facile spectroscopic method for measuring lignin content in lignocellulosic biomass. Green. Chem. 23, 5106–5112.
Lundqvist, J., Jacobs, A., Palm, M., Zacchi, G., Dahlman, O., Stålbrand, H., 2003. Characterization of galactoglucomannan extracted from spruce (Picea abies) by heat-fractionation at different conditions. Carbohydr. Polym. 51, 203–211.
Mänttäri, M., Al Manasrah, M., Strand, E., Laasonen, H., Preis, S., Puro, L., Xu, C., Kisonen, V., Korpinen, R., Kallioinen, M., 2015. Improvement of ultrafiltration performance by oxidation treatment in the recovery of galactoglucomannan from wood autohydrolyzate. Sep. Purif. Technol. 149, 428–436.
Mikkonen, K.S., 2020. Strategies for structuring diverse emulsion systems by using wood lignocellulose-derived stabilizers. Green. Chem. 22, 1019–1037.
Mikkonen, K.S., Heikkilä, M.I., Helén, H., Hyvönen, L., Tenkanen, M., 2010. Spruce galactoglucomannan films show promising barrier properties. Carbohydr. Polym. 79, 1107–1112.
Mikkonen, K.S., Merger, D., Kilpeläinen, P., Murtomäki, L., Schmidt, U.S., Wilhelm, M., 2016. Determination of physical emulsion stabilization mechanisms of wood hemicelluloses via rheological and interfacial characterization. Soft Matter 12 (*42*), *8690–8700*.
Mikkonen, K.S., Kirjoranta, S., Xu, C., Hemming, J., Pranovich, A., Bhattarai, M., Peltonen, L., Kilpeläinen, P., Maina, N., Tenkanen, M., 2019. Environmentally-compatible alkyd paints stabilized by wood hemicelluloses. Ind. Crops Prod. 133, 212–220.
Nypelö, T., Laine, C., Aoki, M., Tammelin, T., Henniges, U., 2016. Etherification of wood-based hemicelluloses for interfacial activity. Biomacromolecules 17, 1894–1901.
Olsson, A.-M., Salmén, L., 1997. The effect of lignin composition on the viscoelastic properties of wood. Nord. Pulp Pap. Res. J. 12, 140–144.
Persson, T., Jönsson, A.-S., 2010. Isolation of hemicelluloses by ultrafiltration of thermomechanical pulp mill process water—Influence of operating conditions. Chem. Eng. Res. Des. 88, 1548–1554.
Roos, Y.H., 2010. Glass transition temperature and its relevance in food processing. Annu. Rev. Food Sci. Technol. 1, 469–496.
Song, T., Pranovich, A., Sumerskiy, I., Holmbom, B., 2008. Extraction of galactoglucomannan from spruce wood with pressurised hot water. Holzforschung 62, 659–666.
Song, T., Pranovich, A., Holmbom, B., 2011a. Characterisation of Norway spruce hemicelluloses extracted by pressurised hot-water extraction (ASE) in the presence of sodium bicarbonate. Holzforschung 65, 35–42.
Song, T., Pranovich, A., Holmbom, B., 2011b. Effects of pH control with phthalate buffers on hot-water extraction of hemicelluloses from spruce wood. Bioresour. Technol. 102, 10518–10523.
Song, T., Pranovich, A., Holmbom, B., 2013. Separation of polymeric galactoglucomannans from hot-water extract of spruce wood. Bioresour. Technol. 130, 198–203.
Steinmetz, V., Villain-Gambier, M., Klem, A., Gambier, F., Dumarcay, S., Trebouet, D., 2019. Unveiling TMP process water potential as an industrial sourcing of valuable lignin–carbohydrate complexes toward zero-waste biorefineries. ACS Sustain. Chem. Eng. 7, 6390–6400.
Stelte, W., Clemons, C., Holm, J.K., Ahrenfeldt, J., Henriksen, U.B., Sanadi, A.R., 2011. Thermal transitions of the amorphous polymers in wheat straw. Ind. Crops Prod. 34, 1053–1056.
Strand E. (2016). Enhancement of ultrafiltration process by pretreatment in recovery of hemicelluloses from wood extracts, Lappeenranta University of Technology, Lappeenranta, Finland.
Sundberg, A., Lillandt, C., Holmhom, B., 1996. Determination of hemicelluloses and pectins in wood and pulp fibres by acid methanolysis and gas chromatography. Nord. Pulp Pap. Res. J. 11, 216–219.
Thuvander, J., Jönsson, A.-S., 2016. Extraction of galactoglucomannan from thermomechanical pulp mill process water by microfiltration and ultrafiltration—Influence of microfiltration membrane pore size on ultrafiltration performance. Chem. Eng. Res. Des. 105, 171–176.
Vallar, S., Houivet, D., El Fallah, J., Kervadec, D., Haussonne, J.-M., 1999. Oxide slurries stability and powders dispersion: optimization with zeta potential and rheological measurements. J. Eur. Ceram. Soc. 19, 1017–1021.
Valoppi, F., Maina, N., Allén, M., Miglioli, R., Kilpeläinen, P.O., Mikkonen, K.S., 2019. Spruce galactoglucomannan-stabilized emulsions as essential fatty acid delivery systems for functionalized drinkable yogurt and oat-based beverage. Eur. Food Res. Technol. 245, 1387–1398.
Wang, C., Zhang, Y., Huang, H.X., Chen, M.B., Li, D.S., 2011. Solution conformation of konjac glucomannan single helix. Adv. Mater. Res. Vol. 197, 96–104.
Willemann, J.R., Escher, G.B., Kaneshima, T., Furtado, M.M., Sant'Ana, A.S., Vieira do Carmo, M.A., Azevedo, L., Granato, D., 2020. Response surface optimization of phenolic compounds extraction from camu-camu (Myrciaria dubia) seed coat based on chemical properties and bioactivity. J. Food Sci. 85, 2358–2367.
Willför, S., Sundberg, A., Hemming, J., Holmbom, B., 2005. Polysaccharides in some industrially important softwood species. Wood Sci. Technol. 39, 245–257.
Willför, S., Sundberg, K., Tenkanen, M., Holmbom, B., 2008. Spruce-derived mannans–A potential raw material for hydrocolloids and novel advanced natural materials. Carbohydr. Polym. 72, 197–210.
Xu, C., Willfor, S., Sundberg, K., Pettersson, C., Holmbom, B., 2007. Physico-chemical characterization of spruce galactoglucomannan solutions: stability, surface activity and rheology. Cellul. Chem. Technol. 41, 51.
Xu, C., Willför, S., Holmbom, B., 2008. Rheological properties of mixtures of spruce galactoglucomannans and konjac glucomannan or some other polysaccharides. BioResources 3 (*3*), *713–730*.
Xu, C., Leppänen, A.-S., Eklund, P., Holmlund, P., Sjöholm, R., Sundberg, K., Willför, S., 2010. Acetylation and characterization of spruce (Picea abies) galactoglucomannans. Carbohydr. Res. 345, 810–816.
Ye, X.-X., Luo, W., Lin, L., Zhang, Y.-q, Liu, M.-h, 2017. Quaternized lignin-based dye dispersant: Characterization and performance research. J. Dispers. Sci. Technol. 38, 852–859.
Zasadowski, D., Yang, J., Edlund, H., Norgren, M., 2014. Antisolvent precipitation of water-soluble hemicelluloses from TMP process water. Carbohydr. Polym. 113, 411–419.